

1 A compact acoustic calibrator for ultra-high energy neutrino detection

2 S. Adrián-Martínez, M. Ardid, M. Bou-Cabo, G. Larosa, C.D Llorens, J.A. Martínez-Mora
3 Institut d'Investigació per a la Gestió Integrada de les Zones Costaneres, Universitat Politècnica de València, C/
4 Paranimf 1, 46730 Gandia, València, Spain.

5
6 Corresponding autor. Tel.: +34 962849314; Fax: +34 962849309
7 E-mail address: siladmar@upv.es (S. Adrián-Martínez)

8
9 **ABSTRACT**

10
11 With the aim to optimize and test the method of acoustic detection of ultra-high energy neutrinos in underwater
12 telescopes a compact acoustic transmitter array has been developed. The acoustic parametric effect is used to reproduce
13 the acoustic signature of an ultra-high-energy neutrino interaction. Different R&D studies are presented in order to show
14 the viability of the parametric sources technique to deal with the difficulties of the acoustic signal generation: a very
15 directive transient bipolar signal with 'pancake' directivity. The design, construction and characterization of the
16 prototype are described, including simulation of the propagation of an experimental signal, measured in a pool, over a
17 distance of 1 km. Following these studies, next steps will be testing the device in situ, in underwater neutrino telescope,
18 or from a vessel in a sea campaign.

19 *Keywords:*

20 Underwater neutrino telescopes; acoustic neutrino detection; parametric acoustic sources; underwater acoustic array
21 sensors.

22
23 1. Introduction

24 The method of acoustic detection is a promising
25 technique for the detection of cosmic neutrinos with
26 energies exceeding 1 EeV. Askariyan in 1957 published
27 the first studies in relation with the possibility of
28 detecting ionizing particles by acoustic techniques [1].
29 When a neutrino interacts with a nucleus of water, a
30 particle shower is generated. On average, 25% of the
31 neutrino energy is deposited in a cylindrical volume of a
32 few cm of radius and several meters of length and it
33 produces an instantaneous, with respect to the
34 hydrodynamic time scales, local heating of the medium.
35 As a consequence of the temperature change and
36 depending on the volume expansion coefficient of the
37 medium, an expansion or contraction of the medium is
38 induced. A pressure pulse of bipolar shape is
39 propagated in the surrounding medium due the
40 accelerated expansion of the heated volume [2-3] with,
41 due to the dimensions of the source, a 'pancake'
42 directivity. This means a flat disk emission pattern
43 perpendicularly to the axis defined by the hadronic
44 shower. As a reference example at 1 km distance in
45 perpendicular direction to a 10^{20} eV hadronic shower, it
46 is expected that the bipolar acoustic pulse has about 0.2
47 Pa (peak-to-peak) in amplitude and about 50 μ s length
48 (peak-to-peak). With respect to the directivity pattern
49 the opening angle of the pancake is expected to be
50 about 1°. Ultra-high energy (UHE) acoustic detection is
51 a promising technique to extend the energy range of
52 different experiments. In that sense, ANTARES [4] is
53 considering the technique, using the detector as
54 platform to test the feasibility of a large-scale acoustic
55 neutrino detector to combine optical and acoustical
56 detection techniques for hybrid underwater neutrino
57 telescopes, especially considering that the optical

58 neutrino technique needs acoustic sensors as well for
59 positioning purposes. ANTARES contains AMADEUS
60 [5], an acoustic test setup which is operational and
61 taking data. It can be considered a prototype to evaluate
62 the feasibility of the neutrino acoustic detection. Even
63 though all AMADEUS sensors have been characterized
64 in the lab, it would be desirable to deploy a compact
65 calibrator that "in situ" may be able to calibrate the
66 detection system, to train and tune the system in order
67 to improve its performance, to test and validate the
68 technique, and to determine the reliability of the system
69 [6].

70
71 2. Previous studies

72 Previous research studies were done to evaluate the
73 possibility of using the parametric acoustic sources
74 technique to reproduce the acoustic signature of a UHE
75 neutrino interaction.
76 Acoustic parametric generation was first proposed by
77 Westervelt [7] in the 1960's. The acoustic parametric
78 effect occurs when two intense monochromatic beams,
79 with two close frequencies, travel together through a
80 medium. Under these conditions, in the region of
81 nonlinear interaction, secondary harmonics of these
82 frequencies are produced: the sum and difference of the
83 frequencies and the double frequencies of both beams.
84 The main advantage of this technique is that the
85 secondary parametric beam has the same directivity
86 pattern as the primary beam, enabling low frequency
87 beams (difference frequency) with high directivity
88 (primary beam). Since the emission is made at high
89 frequencies, it is possible to obtain narrow directional
90 patterns using a transducer with small overall
91 dimensions. However there are some difficulties when
92 applying this method to a compact acoustic calibrator as

93 the neutrino acoustic signal is a transient signal with
 94 broad frequency content with a cylindrically symmetric
 95 directivity. To deal with transient signals, theoretical
 96 and experimental studies [8] indicate that it is possible
 97 to generate a signal with ‘special’ modulation at larger
 98 frequency in such a way that the pulse interacts with
 99 itself while it is travelling through the medium, thereby
 100 generating the desired signal. In this case, the secondary
 101 parametric signal generated in the medium is related to
 102 the second time derivative of the envelope of the
 103 primary signal, following the equation:

$$104 \quad 105 \quad 106 \quad 107 \quad 108 \quad p(x,t) = \left(1 + \frac{B}{2A}\right) \frac{P^2 S}{16\pi\rho c^4 \alpha x} \frac{\partial^2}{\partial t^2} \left[f\left(t - \frac{x}{c}\right) \right]^2$$

109 where P is the pressure amplitude of the primary signal,
 110 S is the surface area of the transducer, $f(t-x/c)$ is the
 111 envelop of the primary signal, x is the propagation
 112 distance, t is the time, B/A the nonlinear parameter of
 113 the medium, ρ is the density, c the sound speed and α is
 114 the absorption coefficient.

115 Our first studies were done in the lab using planar
 116 transducers. This work concluded with positive results
 117 regarding the feasibility of the bipolar pulse generation
 118 with the parametric technique [9].

119 The next step was to deal with the cylindrical
 120 symmetry. A new setup was configured in order to, on
 121 the one hand, study in more detail the influence of the
 122 signal envelope used in emission with respect to the
 123 secondary beam generated in the medium and, on the
 124 other hand, reproducing the desired ‘pancake’ pattern of
 125 emission. For this purpose a single cylindrical
 126 transducer (Free Flooded Ring SX83, (FFR-SX83),
 127 manufactured by Sensor Technology Ltd., Canada) was
 128 used. This work is described in [10] and the results
 129 obtained agreed with the expectations from parametric
 130 theory and previous measurements, but now being able
 131 to generate the signals for almost cylindrical
 132 propagation. Afterwards, new measurements over
 133 longer distances were made in a larger pool using the
 134 same equipment and conditions [11]. The main
 135 objective was to compare the pressure level of both
 136 beams, primary and secondary ones, as a function of the
 137 distance since the difference of the attenuation factors is
 138 clear evidence that confirms the parametric acoustic
 139 generation of the secondary bipolar pulse. In these
 140 measurements, the obtaining of similar directivity
 141 patterns for both beams was also confirmed. An
 142 opening angle with a FWHM of about 14° was
 143 observed.

144 Following these results, the parametric acoustic sources
 145 technique can be considered a good tool to develop a
 146 transmitter able to mimic the acoustic signature of a
 147 UHE neutrino interaction. Moreover, it presents the
 148 advantage of a compact design with respect to other
 149 classical solutions [12]. To obtain directive beams with
 150 a linear phased array, the use of higher frequencies
 151 implies that fewer elements with smaller spatial
 152 separation are needed. Such a device would be easier to
 153 install and deploy in an undersea neutrino telescope.

154
155
156
157
158
159
160
161
162
163
164
165
166
167
168
169
170
171
172
173
174
175
176
177
178
179
180
181
182
183
184
185
186
187
188
189
190
191
192
193
194
195
196
197
198
199
200
201
202
203
204
205
206
207
208
209
210
211
212
213

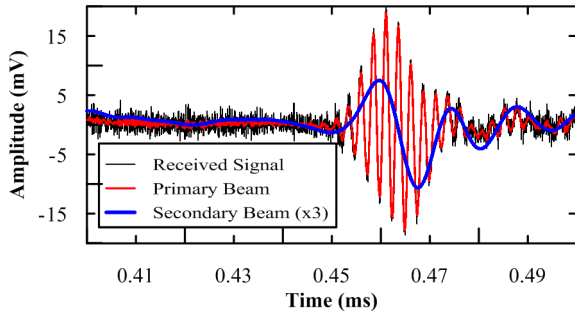
3. Compact acoustic system: design and tests

3.1 First prototype of the compact array

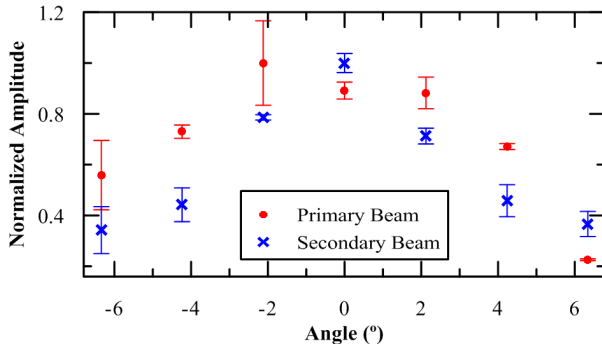
With the aim of reproducing the ‘pancake’ directivity a
 three element array configuration solution is proposed.
 Moreover, the array will improve the signal level of the
 non-linear beam generated at the medium to cover long
 distances. The array is composed of three FFR-SX83
 transducers. Each one has a diameter of 11.5 cm and is
 5 cm height. The transducers usually work in the 5-20
 kHz range, but for our application a second resonance
 peak at about 400 kHz is used, which is the frequency
 used for the primary beam. The array developed for the
 tests has a separation between elements of 2 cm, i.e. the
 active part of the array has a total height of 20 cm. The
 three elements are fixed by three bars with mechanical
 supports to maintain the linear array configuration.
 Measurements for the array characterization have been
 made in a pool of 6.3 m length, 3.6 m width and 1.5 m
 depth. The array is used as emitter, and the receiving
 hydrophone used to measure the acoustic waveforms is
 a spherical omnidirectional transducer (model ITC-
 1042) connected to a 20 dB gain preamplifier (Reson
 CCA 1000). A DAQ system is used for emission and
 reception. To drive the emission, a 14 bits arbitrary
 waveform generator (National Instruments, PCI-5412)
 has been used with a sampling frequency of 10 MHz.
 This feeds a linear RF amplifier (1040L, 400W, +55
 dB, Electronics & Innovation Ltd.) used to amplify the
 emitted signal. For the reception, an 8 bit digitizer
 (National Instruments, PCI-5102) has been used with a
 sampling frequency of 20 MHz. The recorded data are
 processed and band-pass filter (FIR, corner frequencies
 5 kHz and 100 kHz) is applied to extract the secondary
 beam signal, as well as the relevant signal parameters
 (amplitude, shape and duration) to study.

An example of a received signal and the primary and
 secondary beams obtained after applying the band-pass
 filter used are shown on Figure 1 (the secondary beam
 has been amplified by a factor 3 for a better visibility).
 Figure 2 shows the directivity pattern measured along a
 line parallel to the axis of the array at a distance of 2.7
 m. It allows studying the angle distribution of both
 beams. Instead of having for the primary beam a thin
 peak, a wide peak with no clear maximum is observed.
 This is due to the fact that the measurements were done
 at a distance which cannot be considered very large, and
 therefore the signals from the different transducers are
 not totally synchronous at 0° . Moreover, some of the
 variations of the primary beam may be due as well to
 the interference (constructive or destructive) of the
 individual beams, which are not only observed from the
 variations point to point, but even in the same point.
 This might be the reason for the large differences
 observed in the statistical uncertainties of the primary
 beam measures. Despite the small distance, the
 behaviour of the secondary beam is smoother and the
 FWHM measured with the array is about 7° ($\sigma=3^\circ$), that
 is, smaller than for the primary beam, and sensitively

214 smaller than for a single element where the FWHM was
 215 about 14° ($\sigma = 6^\circ$). Moreover, considering that the
 216 signals for the three elements will be better
 217 synchronized at large distances (larger than 100 m), it
 218 seems possible to achieve a ‘pancake’ directivity with
 219 an aperture of the 1^o order ($\sigma \sim 1^\circ$) for large distances,
 220 as expected from our calculations [11].



222
 223 Figure 1. Example of a received signal. Primary and
 224 secondary beams obtained after applying the bandpass
 225 filter (the secondary beam has been amplified by a
 226 factor 3 for a better visibility).

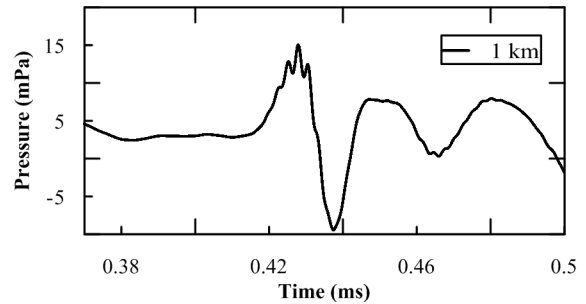


227
 228 Figure 2. Directivity patterns of primary and secondary
 229 beam measured with the array.

231 3.2 Propagation to large distances

232 In order to show the effect of the propagation caused on
 233 the bipolar parametric signal, signals recorded
 234 experimentally have been propagated to a distance of 1
 235 Km. An algorithm which works in the frequency
 236 domain corrects the frequency dependence of the
 237 hydrophone sensitivity and propagates each spectral
 238 component considering the geometrical attenuation of
 239 the pressure beams as $1/r$ and the absorption coefficient
 240 [13] calculated for the sea conditions in the ANTARES
 241 site is used. Figure 3 shows a signal propagated to 1 km
 242 (original signal was measured in the lab with a distance
 243 of 0.7 m). In this case, no additional filter is applied, the
 244 propagation medium acts as a natural filter. To be exact,
 245 there is still a small high-frequency component which is
 246 not observed at distances of 1.2 km (or higher). Notice
 247 that the high-frequency signal was three orders of
 248 magnitude higher than the secondary beam at ~ 1 m
 249 distance. It appears as well a kind of DC offset, it is due
 250 to the very low-frequency components of the signal
 251 (probably 50 Hz) which are also propagated. As
 252 conclusion, using a single element it is expected to have
 253 a bipolar pulse with 25 mPa peak-to-peak amplitude at
 254 1 km distance from the sensor and 0° direction.

255 Considering the array configuration with three elements
 256 feed in phase with the maximum power, which is not
 257 possible with the current electronics, it is expected to
 258 have, at least, 0.1 Pa peak-to-peak, which is a value
 259 clearly above the AMADEUS threshold (20 mPa) [5],
 260 and corresponds to the pressure reference of the order of
 261 a neutrino interaction of 10^{20} eV at 1 km distance.
 262



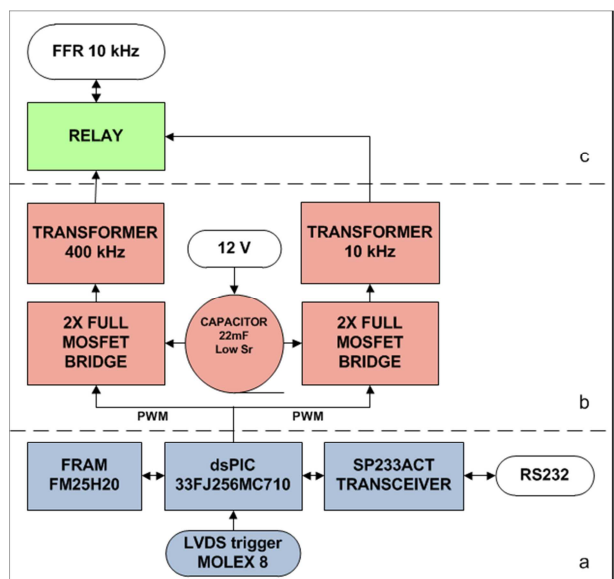
263
 264 Figure 3. Signal obtained after 1 km propagation.

266 3.3 Second prototype of the compact array

267 The final goal is to have a system able to carry out
 268 several tasks related to acoustics in an underwater
 269 neutrino telescope using the same transmitter: acoustic
 270 detection calibration, calibration of the acoustic
 271 receivers sensitivity, and signals emission for
 272 positioning tasks. Certainly, this could reduce the cost
 273 and facilitate the deployment and operation at deep sea.

275 3.3.1 Mechanics

276 For the second prototype the transducers are fixed on a
 277 rigid axis using flexible polyurethane (EL110H, Robnor
 278 Resins Ltd). Due to the nature of the cured polymer,
 279 this offers water resistance and electrical insulation for
 280 high frequency and high voltage applications. The
 281 resulting compact design has a length of 17.5 cm for the
 282 active region. In addition, a mechanical structure has
 283 been built for handling the array from a boat and
 284 controlling its rotation angle (orientation of the
 285 emission). This is a critical aspect to be able to point to
 286 the receivers due to the high directivity.
 287



288

289 Figure 4. Electronics block diagram: Communication
290 and control (a), emission (b) and commuter between the
291 two operation modes (c).

292 3.3.2 Associated electronics

294 Developments in electronics have been made with the
295 aim of having an autonomous and optimized compact
296 system able to work in different frequency ranges for
297 different applications, see Figure 4. An electronic
298 device that controls the transmitter, generates and
299 amplifies the signals in order to have enough acoustic
300 power to achieve the emission in nonlinear regime. This
301 is an essential requirement for parametric generation
302 and it is necessary for calibration and/or positioning
303 purposes in order to be detected from distant acoustic
304 receivers.

305 A novelty in the design is the use of Pulse Width
306 Modulation technique (PWM) [14]. With this, it is
307 possible to emit arbitrary intense short signals, and
308 therefore to emit the necessary ‘modulated signal’ with
309 the goal of obtaining a secondary beam with the desired
310 specifications. This technique has been already
311 implemented for the acoustic transceiver electronics of
312 the positioning systems for the future KM3NeT
313 neutrino telescope [15-17].

314 Some of the advantages this technique offers are:

- 315 • Efficiency: System uses class D amplification.
316 Transistors are working on switching mode,
317 suffering less power dissipation.
- 318 • Simplicity of design: Analogic-digital converters
319 are not needed. It is possible to feed directly the
320 amplifier with the digital signal modulated by the
321 PWM technique.
- 322 • Lightweight and compact system: It is not
323 necessary to install large heat sinks at the
324 amplifier transistors.
- 325 • Minimum power consumption in stand-by mode:
326 this is required for a system of a deep-sea
327 detector. Moreover, it allows storing the energy
328 in the amplifier capacitor very fast and
329 efficiently for using it in the following emission.

331 4. Conclusions and future steps

332 Considering all the results obtained in relation to the
333 studies of parametric acoustic sources and to the first
334 array prototype it seems clear that the solution proposed
335 based on parametric acoustic sources could be
336 considered a good candidate to generate the acoustic
337 neutrino-like signals, with both specific characteristics
338 of the predicted signal: bipolar shape in time and
339 ‘pancake directivity’.

340 Moreover, due to the transmitter system versatility, the
341 array plus the electronics described for the last
342 prototype could be implemented to carry out several
343 tasks related to acoustic emission for underwater
344 neutrino telescopes: positioning, acoustic detection
345 calibration and calibration of the receiver hydrophone
346 sensitivities. This may simplify the set of acoustic
347 transmitters needed in a neutrino telescope, and thus

348 may reduce the complexity of the system and the costs
349 with respect to the use of multiple devices.
350 The future work will consist in completing the compact
351 transmitter prototype (array+electronics) and
352 characterizing it in the lab and in situ. For the last part,
353 tests of the transmitter using the AMADEUS system are
354 foreseen, either using the array from a vessel in a sea
355 campaign or maybe integrated in the ANTARES
356 infrastructure.

358 Acknowledgements

359 This work has been supported by the Ministerio de
360 Ciencia e Innovación (Spanish Government), project
361 references FPA2009-13983-C02-02, ACI2009-1067,
362 Consolider-Ingenio Multidark (CSD2009-00064). It has
363 also being funded by Generalitat Valenciana,
364 Prometeo/2009/26.

367 References

- 368 [1] G.A. Askariyan, J. At. Energy, 3, 1957, 921.
- 369 [2] G.A. Askariyan, B.A. Dolgosheinb, A.N.
370 Kalinovskiyb and N.V. Mokhov, Nucl. Instr. and Meth.,
371 164, 1979, 267-278.
- 372 [3] J.G. Learned, Physical Rev. D, 19, 1979, 3293-
373 3307.
- 374 [4] M. Ageron et al. (ANTARES Collaboration), Nucl.
375 Instr. And Meth. A, 651, 2011, 11-38.
- 376 [5] J.A. Aguilar et al. (ANTARES Collaboration), Nucl.
377 Instr. and Meth. A, 626–627, 2011, 128-143.
- 378 [6] M. Ardid, Nucl. Instr. and Meth. A, 604, 2009,
379 S203-S207.
- 380 [7] P. J. Westervelt, J. Acoust. Soc. Am., 35, 1963,
381 535-537.
- 382 [8] M.B. Moffett and P. Mello, J. Acoust. Soc. Am.,
383 66, 1979, 1182- 1187.
- 384 [9] M. Ardid et al., Nucl. Instr. and Meth. A, 604, 2009,
385 S208-S211.
- 386 [10] M. Ardid et al., Nucl. Instr. and Meth. A, 662,
387 2012, S206-S209.
- 388 [11] M. Ardid et al., Sensors, 12, 2012, 4113-4132.
- 389 [12] W. Ooppakaew et al., IEEE Eighth International
390 Conference on Mobile Ad-Hoc and Sensor Systems,
391 2011, 910-915.
- 392 [13] R.E. Francois, G.R. Garrison, J. Acoust. Soc. Am.,
393 Part I. 72(3), 1982, 896-907. Part II. 72(6), 1982, 1879-
394 1890.
- 395 [14] M. Barr, Introduction to Pulse Width Modulation,
396 Embedded Systems Programming 14,10, 2001,103-104.
- 397 [15] M. Ardid et al., Nucl. Instr. and Meth. A, 617,
398 2010, 459- 461.
- 399 [16] M. Ardid et al., Nucl. Instr. and Meth. A, 626- 627,
400 2011 S214-S216.
- 401 [17] C.D. Llorens, et al., J. Instrum. 2012, 7, C01001
- 402